Numerical Simulation of Flow in Intake Ports and Cylinder of Multi-Valve S. I. Engine using PCC Method

Y.Takahashi, K.Fukuzawa and I.Fujii

EMS Block, Wako Research Center
Honda R&D Co., Ltd.
1-4-1 Chuo, Wako, Saitama 351-01
Japan

ABSTRACT

From the view of engine designers, the need grows for the prediction of three-dimensional in-cylinder flow in realistic engine geometry. Further, the prediction must be made within a limited development time schedule. BFC is widely used for CFD, however, the mesh generation for complicated geometry is difficult and extremely time consuming.

The purpose of this study is to develop an economical CFD code for practical use by reducing the input data preparation. As a result, a new method of Partial Cells in Cartesian coordinate (PCC) has been developed. The input data is prepared by the data of the geometry configuration and by the data of the computational mesh. The two data are individual because their mutual relation is computed in CFD code.

This paper describes implementation of this method and shows prediction results. Comparisons between prediction and measurement are made with the effective valve area, and show good agreement at each valve lift.

INTRODUCTION

The researches of lean burn engines have become important to reduce the emission and the fuel consumption per cylinder through swirl or tumble. However, the gas motion has not been fully analyzed, so many experiments are employed with many trial productions of intake ports and combustion chambers to develop engines. By the rapid progress of computer performance, the three-dimensional computational fluid dynamics (CFD) has become applicable to engine analysis[1][2][3]. Moreover, CFD is expected as one of the influential analysis method in the near future.

At present, Boundary Fitted Coordinates (BFC) are widely used due to the benefit in shape expression. However, BFC has large problems when applied to the complicated geometry associated with engines. The problems stem from the preparation of three-dimensional input data, which requires many operations and technical skills. Therefore, within a short engine development period, analysis is limited to the number of various engine configurations. Otherwise, analysis is made with simple geometry. Although CFD has a few benefits for engine development, the cost including personnel expense is expensive. There are some approaches to reduce the time of mesh generation. One example is the improvement of mesh generation method, and another is the use of an unstructured mesh. It appears that mesh generation is an important theme.

On the other hand, in the progress of CFD, partial cells were used to express an object geometry with two-dimensional FLIC method[4]. The primary advantage of partial cells is easy mesh generation. Recently, a porosity technique was applied to three-dimensional flow in engine intake ports[5][6], and Cartesian coordinates have been reconsidered among CFD researchers.

From the view of CFD users, the ideal image for input data is as follows. The data of geometry configuration and the data of computational mesh can be prepared separately because their mutual relation is computed in CFD code.

The purpose of this study is to develop an economical CFD code for practical use by reducing input data preparation. As a result, a new method with Partial Cells in Cartesian coordinate (PCC) has been developed. This paper describes implementation of this method and shows prediction results using a four-valve SI engine under a steady state condition of a flow rig test. Comparisons between prediction and measurement are made with the effective valve area, and show good agreement at each valve lift.

GOVERNING EQUATIONS

The mass conservation, the momentum equations (Navier-Stokes equation) and the standard k-ε turbulence model[7] in Cartesian coordinate are expressed as follows:

[mass conservation]

$$\frac{\partial \rho}{\partial t}+\frac{\partial(\rho u)}{\partial x}+\frac{\partial(\rho v)}{\partial y}+\frac{\partial(\rho w)}{\partial z}=0 \qquad (1)$$

[x direction momentum equation]

$$\frac{\partial(\rho u)}{\partial t}+\frac{\partial(\rho uu)}{\partial x}+\frac{\partial(\rho vu)}{\partial y}+\frac{\partial(\rho wu)}{\partial z}+\frac{\partial p}{\partial x}$$

$$= \frac{\partial}{\partial x}(\mu_e \frac{\partial u}{\partial x}) + \frac{\partial}{\partial y}(\mu_e \frac{\partial u}{\partial y}) + \frac{\partial}{\partial z}(\mu_e \frac{\partial u}{\partial z}) + \frac{1}{3}\frac{\partial}{\partial x}(\mu_e(\frac{\partial u}{\partial x} + \frac{\partial v}{\partial y} + \frac{\partial w}{\partial z})) - \frac{2}{3}\frac{\partial(\rho k)}{\partial x} \quad (2)$$

where, $\mu_e = \mu + \mu_t = \mu + C_\mu \rho \frac{k^2}{\varepsilon}$ (3)

The momentum equations in y and z direction are expressed similarly to the above equation.

[turbulence kinetic energy]

$$\frac{\partial(\rho k)}{\partial t} + \frac{\partial(\rho u k)}{\partial x} + \frac{\partial(\rho v k)}{\partial y} + \frac{\partial(\rho w k)}{\partial z} = \frac{\partial}{\partial x}(\frac{\mu_t}{\sigma_k}\frac{\partial k}{\partial x}) + \frac{\partial}{\partial y}(\frac{\mu_t}{\sigma_k}\frac{\partial k}{\partial y}) + \frac{\partial}{\partial z}(\frac{\mu_t}{\sigma_k}\frac{\partial k}{\partial z}) + P_k - \rho\varepsilon \quad (4)$$

where,

$$P_k = 2\mu_t((\frac{\partial u}{\partial x})^2 + (\frac{\partial v}{\partial y})^2 + (\frac{\partial w}{\partial z})^2) + \mu_t((\frac{\partial w}{\partial y} + \frac{\partial v}{\partial z})^2 + (\frac{\partial u}{\partial z} + \frac{\partial w}{\partial x})^2 + (\frac{\partial v}{\partial x} + \frac{\partial u}{\partial y})^2) - \frac{2}{3}\mu_t(\frac{\partial u}{\partial x} + \frac{\partial v}{\partial y} + \frac{\partial w}{\partial z})^2 - \frac{2}{3}\rho k(\frac{\partial u}{\partial x} + \frac{\partial v}{\partial y} + \frac{\partial w}{\partial z}) \quad (5)$$

[eddy dissipation rate]

$$\frac{\partial(\rho\varepsilon)}{\partial t} + \frac{\partial(\rho u\varepsilon)}{\partial x} + \frac{\partial(\rho v\varepsilon)}{\partial y} + \frac{\partial(\rho w\varepsilon)}{\partial z} = \frac{\partial}{\partial x}(\frac{\mu_t}{\sigma_\varepsilon}\frac{\partial\varepsilon}{\partial x}) + \frac{\partial}{\partial y}(\frac{\mu_t}{\sigma_\varepsilon}\frac{\partial\varepsilon}{\partial y}) + \frac{\partial}{\partial z}(\frac{\mu_t}{\sigma_\varepsilon}\frac{\partial\varepsilon}{\partial z}) + \frac{\varepsilon}{k}(C_1 P_k - C_2\rho\varepsilon) \quad (6)$$

where, x, y, z: coordinate axis; t: time; u, v, w: velocity of x, y, z direction, respectively; p: pressure; k: kinetic turbulence energy; ε: eddy dissipation rate; μ_e: effective viscosity; μ: viscosity of air; μ_t: turbulence viscosity; ρ: density; C_μ, C_1, C_2, σ_k, σ_ε: turbulence model constants as follows:

C_μ	C_1	C_2	σ_k	σ_ε
0.09	1.44	1.92	1.0	1.3

PCC METHOD

The PCC method is aimed to calculate fluid under complex object shapes in Cartesian coordinate whenever a mesh line does not consist with an object surface. Thus, partial cells adjacent to the wall are used in CFD code.

Fig. 1 shows the conception of input data. With BFC, the merged input data of geometry configuration and computational mesh is required. On the other hand, with PCC method, the data of computational mesh is separate from the geometry configuration. The geometry data is a solid model created by a 3D-CAD system, for example CATIA. The data consists of facets over the surface, and the

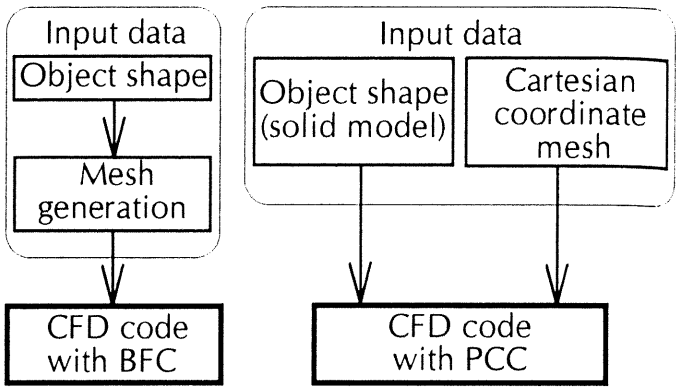

Fig. 1 Comparison of data flow between BFC and PCC

shapes of partial cells are computed from the geometry data in CFD code. For example, cell face areas are obtained by getting cross points between computational mesh lines and facets and calculating triangular areas.

A partial cell is a fluid cell with missed portions by walls from a hexahedron, so many kinds of shapes appear as shown in Fig. 2. For the accuracy of object shape expression, the partial differential equations must be solved with exact response to any resultant shapes of partial cells. Therefore, the discretization equations must be derived based on a finite volume method (FVM).

To predict a gas motion through intake ports with valves and in a cylinder with comparatively fewer mesh numbers, the standard k-ε turbulence model is employed. In this paper, calculations are conducted under a steady state condition of a flow rig test. Incompressible flow is assumed because the pressure difference between inlet and outlet is given as 4kPa.

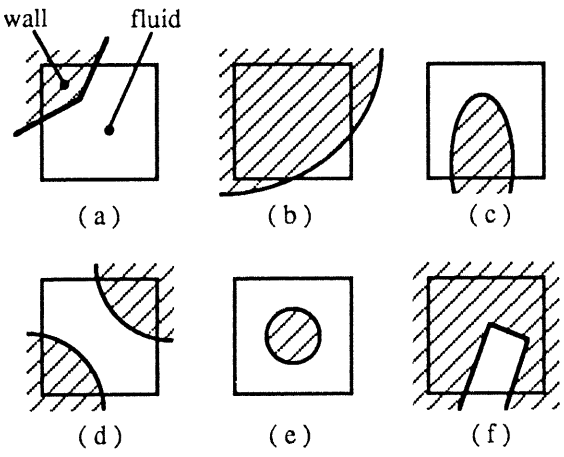

Fig. 2 Examples of partial cells

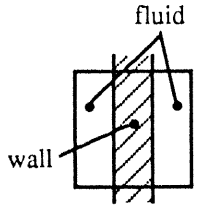

Fig. 3 Excepting divided cells from partial cells

The SIMPLE algorithm[8] is employed among implicit algorithm to keep a large time step in partial cells. The time step is set at infinity for the steady state condition. The hybrid scheme is used for convection and diffusion term. The features of PCC method are:

(1) exact discretization in partial cells, and

(2) boundary condition for the turbulence model.

Note that, in this PCC method, all shapes of partial cells as shown in Fig.2 are considered. However, a divided cell as shown in Fig. 3 is omitted. The reason is that there is only one state of a variable in a cell.

DISCRETIZATION

Fluxes of convection and diffusion

Fig. 4 shows a portion of computational mesh. The integration of the momentum equation for an interior region cell (Fig. 4(a)) and for a partial cell (Fig. 4(b)) becomes as follows:

$$\frac{\rho_P u_P - \rho_P^0 u_P^0}{\Delta t} V + J_e - J_w + J_n - J_s + J_t - J_b = S V \quad (7)$$

where, J is integrated total fluxes (convection plus diffusion) over the cell faces: for example, J_e is defined by the following equation:

$$J_e = \int_e (\rho u u - \Gamma \frac{\partial u}{\partial x}) dA \cong (\rho u u - \Gamma \frac{\partial u}{\partial x})_e A_e \quad (8)$$

S: source term with pressure term; V: actual cell volume; $\rho^0 u^0$: the old (given) values at time t; Γ: effective diffusion coefficient; A: actual cell face area. Note that subscript P shows the cell under consideration; and e, w, n, s, t and b denote cell faces as shown in Fig. 4.

In the conventional FVM, a cell face area A and a cell volume V are simply defined as follow:

$$A_e = A_w = \Delta y \Delta z \qquad V = \Delta x \Delta y \Delta z \quad (9)$$

However, in PCC method, A is an actual area that the flux passes straight through and V is an actual volume occupied by fluid. These A and V values are calculated from the objects. Consequently, whenever the discretization equations in this PCC method are similar to those in the conventional FVM, the integrated values respond to the object shapes through these A and V.

Simultaneously, the mass conservation equation is also integrated using actual cell face areas and actual cell volumes.

Pressure term

The discretization equation of the x direction momentum equation is derived as follow:

$$a_P u_P = a_E u_E + a_W u_W + a_N u_N + a_S u_S + a_T u_T + a_B u_B + S' V - \int (\frac{\partial p}{\partial x}) dV \quad (10)$$

where, a: neighbor coefficient; S': source term without pressure term. Note that the subscript E, W, S, N, T and B express the neighbor cells as shown in Fig. 4.

The pressure force on a hexahedron momentum cell as

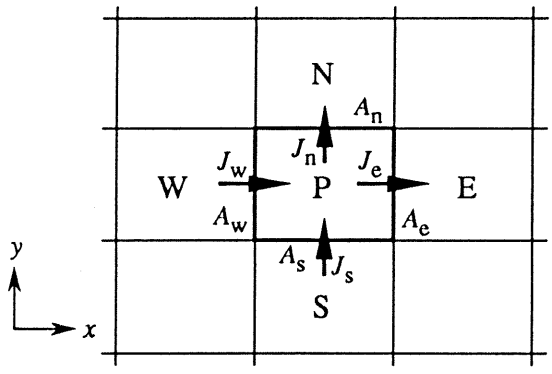

(a) in hexahedron cells

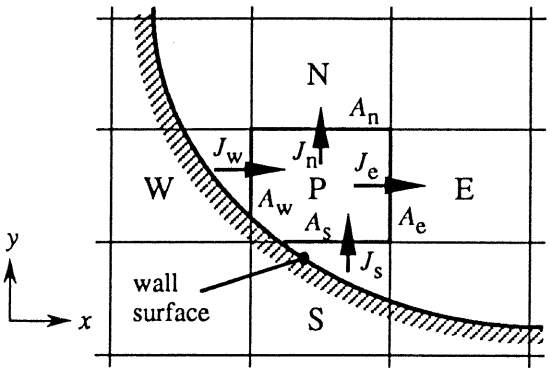

(b) in partial cells adjacent to walls

Fig. 4 Fluxes of convection and diffusion

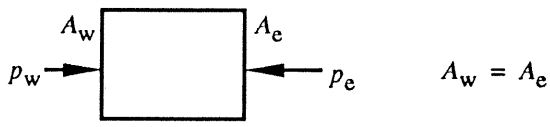

(a) in hexahedron cells (u cell)

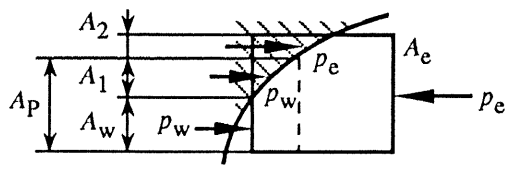

(b) in partial cells (u cell)

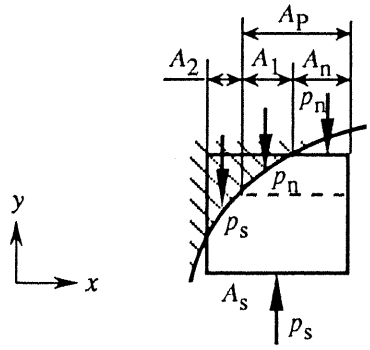

(c) in partial cells (v cell)

Fig. 5 Assumption of pressure distribution

shown in Fig. 5(a) is expressed by the pressure p_e and p_w, and the cell face area A_e and A_w. Therefore, the following equation is obtained:

$$\int (\frac{\partial p}{\partial x}) dV \cong (p_e - p_w) A_P \tag{11}$$

where, $A_P = A_e = A_w$

In partial cells, A_e is not necessarily equal to A_w and the pressure force on the wall must be considered. So an assumption is needed for the pressure distribution in momentum partial cells. Thus, dividing a cell into two parts, the pressure in the west side half-cell is assumed to be equal to the pressure on the west face p_w; and the pressure in the east side half-cell is assumed to be equal to the pressure on the east face p_e. In Fig.5(b), the pressure term is expressed by the following equation:

$$\int (\frac{\partial p}{\partial x}) dV \cong p_e A_e - p_w A_w - p_w A_1 - p_e A_2 \tag{12}$$

where, A_1 and A_2 are projected areas on the wall to x direction. Defining A_p as the area at the interface position between p_e and p_w, the following equation is obtained:

$$A_P = A_w + A_1 = A_e - A_2 \tag{13}$$

thus,

$$\int (\frac{\partial p}{\partial x}) dV \cong (p_e - p_w) A_P \tag{14}$$

Equation (14) is equal to equation (11), therefore, the discretization equation for hexahedron cells and for any shapes of partial cells becomes as follows:

$$\begin{aligned} a_P u_P = {} & a_E u_E + a_W u_W + a_N u_N + a_S u_S \\ & + a_T u_T + a_B u_B + S' V - (p_e - p_w) A_P \end{aligned} \tag{15}$$

In addition, though A_p can be located in any place between A_e and A_w, the value must be calculated exactly from the objects. In the case of v (Fig. 5(c)) and w, the pressure treatment is the same as above.

To avoid a checkerboard pressure field and to satisfy the assumption of the pressure distribution, the staggered grid is employed.

BOUNDARY CONDITIONS

As a boundary condition for the momentum equations and for the turbulence model, the following equations are applied to partial cells from among the wall function[9][10].

$$\tau_w = C_\mu^{1/2} \rho k \tag{16}$$

$$\varepsilon = \frac{C_\mu^{3/4} k^{3/2}}{\kappa y} \tag{17}$$

where, τ_w: wall shear stress; κ: von Kármán constant, 0.42; y: distance from wall to cell center, derived by divided cell volume by wall surface area[5].

PREDICTION RESULTS

The air motion through the intake ports with valves and in the cylinder of a four-valve SI engine is calculated under a steady state condition of a flow rig test. Table 1 shows specifications for the calculation.

Table 1 Specifications for calculation

Cylinder bore	ϕ66mm
Inlet valve diameter (both valves)	ϕ23mm
Valve lift	0 ~ 10mm
Pressure difference between inlet and outlet	4kPa
Number of total cells	44,000
Active cells (at 10mm valve lift)	16,967
Partial cells (at 10mm valve lift)	5,988
CPU time (at each valve lift)	about 90 min.
Computer and the performance by LINPACK benchmark n=100 [11]	IBM RS6000/550 27MFLOPS

Fig. 6 shows the computational mesh and Fig. 7 shows the solid model for the input data. The computational mesh indicates boundary faces of pressure cells with an object outline. Fine meshes are employed around the valves to analyze the flow in detail. On the other hand, larger meshes are used in the ports and the cylinder to save CPU time. The figure shows that the aspect ratio of cells is somewhat large, however, the computation is very stable. Even if a part of an intake port shape or a valve lift is changed, mesh revising is not needed. Consequently, preparations of input data are extremely convenient.

The CPU time is about 90 minutes from the reading of the solid model (Fig. 7) to the output (Fig. 8) in each valve lift

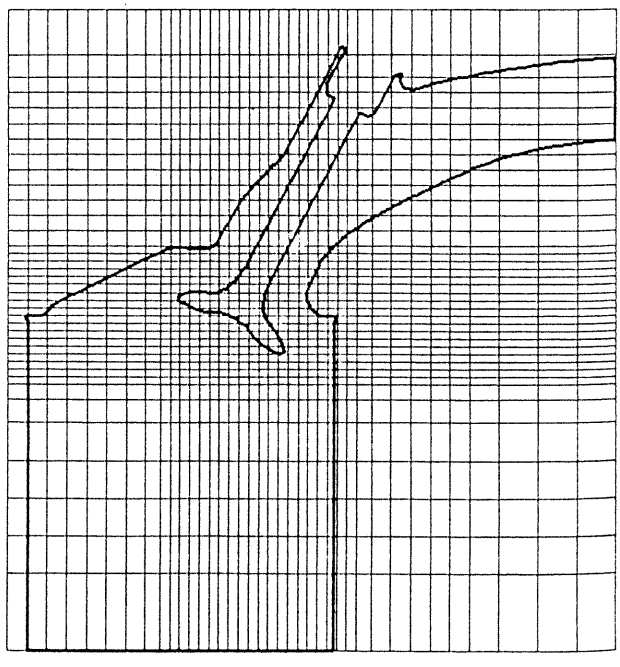

Fig.6 Computational mesh

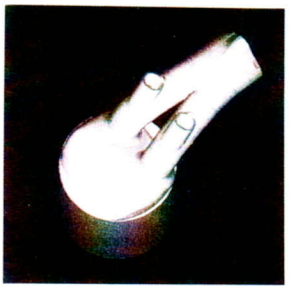

Fig.7 Solid model for calculation

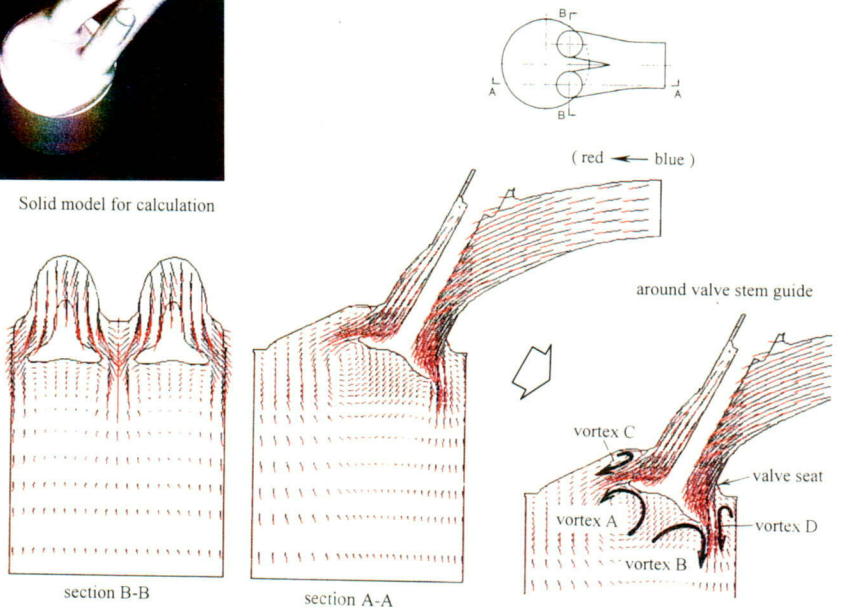

Fig.8 Velocity vectors

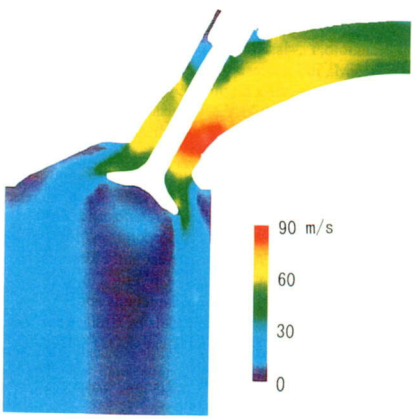

Fig.9 Velocity magnitude

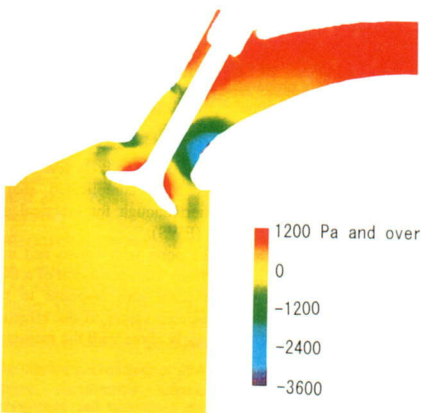

Fig.10 Pressure distribution

using the engineering work station (EWS), IBM RS6000/550. The CPU time includes calculating cell volumes and cell face areas in partial cells from the solid model and solving the flow. There is no interruption such as correcting data of the cell volumes or the cell face areas. The CPU time has been short enough for practical use, since the EWS was introduced on the market in 1991. At present, this code is able to run under personal computers with Intel-486DX2.

Figs. 8 and 9 show velocity vectors and velocity magnitude respectively. These figures show the large vortexes A and B under the valves due to the flow separation at valve edges. Furthermore, the flow separation at the valve seat and the vortexes C and D are observed. At the narrow portion such as the valve stem guide, the prediction shows response to the object shape. Fig. 10 is a pressure distribution, and depicts low pressure at high velocity and at vortexes.

Fig. 11 shows comparisons between the predicted and measured values of the effective valve area (Z) based on valve lift. The definition of Z is as follows[12]:

$$Z = \frac{\dot{m}}{\sqrt{2\rho\Delta p}} \tag{18}$$

where, $\dot{m}$: mass flow rate though the ports; Δp: pressure drop over ports.

The valve lifts are changed by replacement of the solid model. The computational mesh is the same in each valve lift shown in Fig. 6. The predicted values almost agree with the measured values.

In particular, computation around 0 mm valve lift can be conducted by PCC method without additional treatment. Accordingly, predictions in the intake and exhaust stroke may be easy to operate based on exact valve lifts and even at closing point.

CONCLUSIONS

The following conclusions are made by developing a CFD code with the new Partial Cells in Cartesian coordinate (PCC) method for complicated shape objects.

(1) The input data preparation has been extremely convenient because the data of computational mesh is separated from the data of geometry configuration. Therefore, the time consuming jobs are reduced.

(2) The prediction is possible with comparatively fewer mesh numbers even if the objects have complicated shapes. Consequently, CPU time is short enough for practical use with engineering work stations (EWS).

(3) The gas flow through intake ports with valves and in a cylinder is calculated under a steady state condition of a flow rig test. The result shows quite well response to the geometry. As proven, the predicted values of the effective valve area based on valve lift nearly agree with the measured values.

ACKNOWLEDGMENT

The authors would like to express their appreciation to Professor Yuzuru Shimamoto, Associate professor Tomoyuki Wakisaka, University of Kyoto, Associate professor Yoshihiro Isshiki, Setsunan University, and Emeritus professor Tsuyoshi Asanuma, University of Tokyo, for supplying valuable advice during this study.

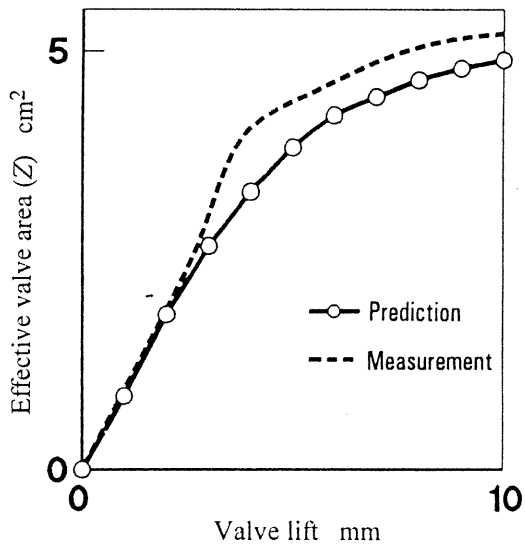

Fig.11 Comparisons between predicted and measured values of the effective valve area

REFERENCES

1. Amsden,A.A., O'Rourke, P.J. and Butler, T.D., Los Alamos National Laboratory report LA-11560-MS (1989)
2. Wakisaka,T., Shimamoto,Y., Isshiki,Y., Sumi,N., Tamura,K. and Modien,R.M., International Symposium COMODIA 90, 487-492 (1990)
3. Naitoh,K., Fujii,H., Urushibara,T., Takagi,Y. and Kuwahara,K., SAE paper 900256 (1990)
4. Gentry,R.A., Martin,R.E. and Daly,B.J., Journal of Computational Physics, Vol.1, 87-118 (1966)
5. Shimamoto,Y., Isshiki,Y., Wakisaka,T. and Uedera,M., in Japanese, 7th Joint Symposium on Internal-Combustion Engine, 397-402 (1988)
6. Shimamoto,Y., Isshiki,Y., Wakisaka,T. and Uedera,M., in Japanese, transactions of JSME (B) Vol.55, No.518 (1989)
7. Patel,V.C., Rodi,W. and Scheuerer,G., AIAA Journal, Vol.23, No.9 (1985)
8. Patankar,S.V., "Numerical Heat Transfer and Fluid Flow", Hemisphere Publishing Corporation (1980)
9. JSME, "Numerical Analysis of Heat and Flow", in Japanese, CORONA Publishing Co.,Ltd. Tokyo (1986)
10. Chen,C.J. and Tanaka,N., "Fundamentals and Applications of Turbulence Models by Ching-Jen-Chen and Nobukazu Tanaka", in Japanese, KOZOKEIKAKU Engineering Inc. Tokyo (1992)
11. Dongarra,J.J., Supercomputing Review, Vol.5, No.3 (1992)
12. Hasegawa,S. and Takahashi,Y., SAE paper 885101(1988)